

Narrowband, Fast, and Autonomous Drone Radio Mapping for Localization

Paul S. Kudyba and Haijian Sun

School of Electrical and Computer Engineering, University of Georgia, Athens, GA, USA

paul.kudyba@uga.edu, hsun@uga.edu

Abstract—This paper explores how a flying drone can autonomously navigate while constructing a narrowband radio map for signal localization. As flying drones become more ubiquitous, their wireless signals will necessitate new wireless technologies and algorithms to provide robust radio infrastructure while preserving radio spectrum usage. A potential solution for this spectrum-sharing localization challenge is to limit the bandwidth of any transmitter beacon. However, location signaling with a narrow bandwidth necessitates improving a wireless aerial system’s ability to filter a noisy signal, estimate the transmitter’s location, and self-pilot toward the beacon signal. By showing results through simulation, emulation, and a final drone flight experiment, this work provides an algorithm using a Gaussian process for radio signal estimation and Bayesian optimization for drone automatic guidance. This research supports advanced radio and aerial robotics applications in critical areas such as search-and-rescue, last-mile delivery, and large-scale platform digital twin development.

Index Terms—Radio Mapping, Gaussian Process, Wireless Localization, Autonomous Aerial Robotics

I. INTRODUCTION

Advances in aerial robotics give engineers new opportunities to collect radio information with a much increased speed and cost efficiency [1]. Within this revolution in capability lies unique engineering insights that could prove foundational to providing the next generation of wireless infrastructure. Such insights are already well established as areas of active wireless research, such as efficient and accurate radio cartography and radio mapping, which can be used to drive improved communication coverage and spectrum occupancy [2]. Furthermore, radio data, once collected or during collection, can be used to drive further valuable inferences, such as transmitter location [3]. However, these spatial radio mapping techniques rely on broadband transmissions, leaving the receiver to decompose the channel response, which compounds the effects of large- and small-scale fading [1], [4]. In contrast to a broadband transmitter, an extremely narrowband transmission (ratio of bandwidth to carrier frequency $\ll 1$) can be leveraged to simplify the channel modeling, but also increase the spectrum efficiency of a localization inference. These combined radio mapping and localization inferences can be used in applications such as last-mile delivery, search-and-rescue, and development of digital twins [5].

A common element in many of these radio insights and inferences is the societal demand to simultaneously produce novel radio technologies and robust standards as infrastructure [6]. This nexus of aerial robotics, wireless technology and

machine learning allowing for researchers to explore new solution spaces and gain new insights, that can in turn, create new radio algorithm frameworks to be easily and rapidly deployed after thorough testing. Our experiment used the Aerial Experimentation and Research Platform for Advanced Wireless (AERPAW) to quickly iterate our algorithm design within an emulated digital twin environment and collect real-world data on the testbed.

This paper brings forward a combined system implementation of aerial mobility, Software-Defined Radio (SDR), and machine learning into a fully deployable top-level algorithm that uses a Gaussian Process (GP) to produce a nonparametric 2D tomographic narrowband channel radio map to be deployed on AERPAW. This radio map is generated as the rover collects samples to form a GP best approximation, or surrogate, of the unknown radio map spatial field. Bayesian Optimization (BO) is then leveraged to infer a best next location to collect a new radio sample. A pipeline methodology was created to simulate robot behavior with various pathloss functions, noise, and BO Activation Functions (AF). A laboratory testbed was constructed to provide signal analysis on the narrowband receiver and develop a filter to reject the deep fading encountered. A final algorithm was then coded to include all previous heuristics and analysis to run within the AERPAW emulator and testbed.

The rest of the paper is structured as follows: in Section I-A, the impetus challenge which supported much of this effort is described. In Section I-B, a general structure of GP and how it is used to construct an evolving radio map as samples are collected. Section I-C gives a relation to how the kernel function and its optimization impact the GP radio map. Section I-D shows how once the GP has established a pathloss gradient, inference can be determined with BO. The methods used to create and deploy the final algorithm are established in Section II with the results shown in Section III. Finally, concluding remarks are given in Section IV.

A. AERPAW Find A Rover Challenge

Participation in the first AERPAW challenge provided an opportunity to address some of the active research questions mentioned above. The goal of the challenge was to use the platform emulator and testbed to locate a rover within three and ten minutes across an area of 19.7 acres using only a repeating BPSK pseudorandom pilot at 3.24 GHz with a 125 KHz bandwidth. A USRP B-210 mini SDR with a

radio front end and filters was used. The objective was to provide the best (lowest) mean error in three randomly chosen locations. Drone log estimates determined two results at the three- and ten-minute, marked from takeoff. Figure 1 illustrates the boundaries and each of the final locations of the rover transmitter. The final submissions were qualified by running them within the AERPAW emulator. If the emulator showed safe flight operation, the algorithm was used on the testbed to determine the final result.

To facilitate radio-based localization, the AERPAW team provided a channel-sounding script that used GNU Radio to interface with the SDR. This script ran a cross-correlation with the transmitted pseudorandom pilot and provided an output channel power in dB and a normalized SNR quality value.



Fig. 1: This figure shows the AERPAW boundaries for the AFAR challenge. The blue indicates the aerial vehicle boundary limits. The green indicates the possible locations of the rover. The numbered red points indicate where the rover was hidden. Similar to Fig. 1 of [7]. The white waypoints indicate the locations sampled within the startup routine for each run.

B. Gaussian Process for Spatial Coverage Radio Mapping

Kriging, emerging from practical use in geostatistics, was formalized into a canonical method called Gaussian Process (GP) [8]. As is used here, a typical application employs a time-invariant surrogate spatial field mapping as stochastic processes or a Gaussian distribution of functions. The effectiveness of reducing a time dimension in a geostatistical context can be easily apparent by producing a cartography or spatial map. However, this particular dimension reduction assumption (e.g., a time-invariant channel) can cause issues in a mobility context. Knowingly, we use a more traditional movement-agnostic signal-processing receiver provided by AERPAW. Nevertheless, this exercise remains important in elucidating an assumption of static dimensionality in a novel system design context and its upstream implications for the system inference

task. Any channel impairment processes not directly accounted for within the receiver design must be considered noise for upstream system insights. This includes temporal noise, such as multipath, Doppler, and sample jitter; even if these alone are relatively small noise sources, they are combined noise sources within our receiver.

In this sense, the radio map we construct will disregard the time-varying aspect of a channel for a direct spatial alignment with radio communication as coverage. This is especially important for mobile communications, where a channel can rapidly encounter fluctuations attributable to many environmental and systemic processes, and having knowledge of such mapping priors can inform downstream reasoning for throughput estimation in a space and time-critical context.

The channel process p_i is a 2D spatial field radio map consisting of a GP with additive noise as shown in Eq. 1. The GP itself describes a probability distribution over a set of radio map functions $f(\cdot)$ shown in Eq. 2 and is characterized by a mean and covariance (or kernel) function. From the domain \mathcal{X} , a 2D spatial distribution prior $f(\cdot)$ is described with a mean function $m(\cdot) = c$ and a covariance function or kernel $k(\cdot, \cdot)$. In this context c is a constant representing the default channel gain corresponding to no signal or receiving incoherent noise. These process descriptor functions (μ, k) correspond to a high-level prior over which the entire GP distribution of functions can resemble.

$$\underbrace{p_i}_{\text{channel process}} = \underbrace{f(\mathbf{X}_i)}_{\text{GP}} + \underbrace{v_i}_{\text{Gaussian noise}} \quad (1)$$

$$f(\cdot) \sim \mathcal{GP}(m(\cdot), k(\cdot, \cdot)) \quad (2)$$

A vector of radio channel estimations, \mathbf{X}_i , is sampled at locations within the domain $\mathcal{X} \subset \mathbb{R}^2$. In our case, the prior $f(\cdot)$ resembles a pathloss, and our expectation is that it should match an exponential decay, but the actual decay exponent remains an unknown parameter (due to the novel system and environment). Thus, this pathloss exponent will be found at run-time as a hyperparameter.

With the correct kernel and hyperparameters, the true spatial field channel, p_i , will be drawn from the GP distribution of radio maps as the mean. This regression, with a prior indicating the most probable radio map and associated uncertainty, is how we generate a rigorous and robust atemporal channel estimate map. Additionally and intuitively, the location of the signal peak within the most probable radio map, when all the dimensional reduction assumptions and noise rejections hold, is the true transmitter's location.

C. Kernel Functions and Maximum Likelihood Algorithm

The kernel function $k(\cdot, \cdot)$ serves as a unified covariance between the prior functions $f(\cdot)$. In this case, the spatial relationships $k(\mathbf{X}, \mathbf{X}')$ correspond to increasing uncertainty as the distance increases from the channel samples. The kernel function must be positive and semi-definite. In this case, the

commonly used Squared Exponential (SE) kernel function is applied as a prior.

$$k_{\text{SE}}(x, x') = \sigma^2 \exp\left(-\frac{(x - x')^2}{2\ell^2}\right) \quad (3)$$

This inherently produces a distribution of infinitely smooth functions that exponentially decay as expected from any free space pathloss function. However, the SE, used alone, would also fit any noise and apply its effects incorrectly to the posterior as part of the pathloss. Fortunately, kernels can be combined with other kernels because they are positive semi-definite. With the addition of a Gaussian noise or white noise kernel, each posterior sample will now account for a hyperparameter of noise within each sample collected, allowing the entire radio map distribution to have more flexibility for inconsistencies in the input sampling. Combined, the starting kernel code is given as `kernel = (C(1) * RBF(0.00276, (0.001, 0.004)) + WhiteKernel(noise_level=0.33)`. This shows a Rational Basis Function (RBF), another name for the SE, with a ℓ value of 0.00276 being bounded between 0.001 and 0.004.

Each kernel comes with a specific set of hyperparameters, which require marginal likelihood optimization to ensure a correct fit that balances the complexity across all the samples collected. For example, the SE kernel requires two hyperparameters σ , a scaling factor, and ℓ called the 'lengthscale' seen in Eq. 3. These hyperparameters are optimized via the Limited-memory Broyden-Fletcher-Goldfarb-Shanno with Bound constraints (L-BFGS-B) algorithm. In this case, the bounding is used to ensure an applicable resulting lengthscale at all times during the flight.

D. Navigation with Bayesian Optimization

The resulting radio map is a distribution of functions and does not have a closed-form solution. Another consideration is the time penalty, opportunity cost, or regret to produce a reliable sample [9]; the drone simply cannot sample the entire field, and yet it needs to know the best next location to fly towards and sample. The GP is also very likely to change as samples are added, especially at the beginning of any flight. These properties disallow many traditional forms of optimization; however, because our radio map has an associated uncertainty provided by our GP kernel function, Bayesian Optimization (BO) can be used to provide an optimal future sample location. This future optimal location will be provided with a closed-form surrogacy from which a maximum can be chosen from the GP output's mean (μ) and uncertainty (σ). BO does this by using an Activation Function (AF), to balance the objective of finding the global optimal by exploration of uncertain positions (exploration), and the best known mean (exploitation).

$$\text{UCB}(X, \Gamma_n) = \mu(X) + \Gamma_n * \sigma(X) \quad (4)$$

Equation 4 gives the activation function used in the final AFAR implementation. It is known as the Upper Confidence

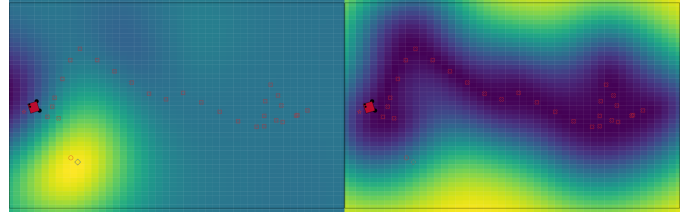


Fig. 2: This figure shows the final results of a robotarium trial showing the GP mean (left) similar to Fig. 4a of [7], and the GP uncertainty as a mean squared error (right). Yellow is a high value, and blue is a low value.

Bound (UCB). Γ is a non-negative exponentially decreasing sequence updated after collecting each sample. Therefore, $\Gamma_n = d^s$, where $0 > d > 1$. This, in effect, reduces the exploration term as the flight progresses and samples are taken.

II. EXPERIMENTAL METHODOLOGY

The production of a final AFAR submission consisted of three stages of research and development: simulation via Robotarium [10], receiver testing with an in-lab setup, and emulation with AERPAW. The results of each stage gave valuable insight into the next building into a cohesive and successful deployment.

A 2D robotic simulator was used to analyze the expected self-guided robot behavior in controlled scenarios, and a path loss functionality was added to facilitate autonomous development. For example, a 2D normal distribution as a basic pathloss function allowed control of the mean as a transmitter's location and the standard deviation to control the decay. The platform enabled many tests with varying pathloss models and signal-to-noise levels. It was also seen that two predefined routines before and after autonomous BO were beneficial to stability, efficiency, and accuracy. The robot would start with a predefined circle routine wide enough to establish a stable gradient and resolve any noise for BO to give stable guidance. Secondly, after a stable global maximum was repeatedly chosen as the optimal location, a routine could be triggered to circle that point, further refining the transmitter's location. Lastly, the simulation allowed experimentation with different AF, leading to the selection of UCB for the final deployment. Figure 2 shows the mean and uncertainty radio maps resulting from BO with uniform noise added to the robot's receiver. A 2D grid was constructed to facilitate getting discrete spatial field points of the GP mean and maximum squared error. The AF could be computed from this grid, and the maximum would then be selected as the new target waypoint.

To ensure that the GP receives no outlier radio data that could not be described as Gaussian noise, a non-linear filter was shown to be necessary from laboratory testing and data from a previous testbed run. A large discriminator was observed by binning the receiver quality signal and taking the variance of these readings. By removing any readings with an excessive quality-variance, large signal noise swings could

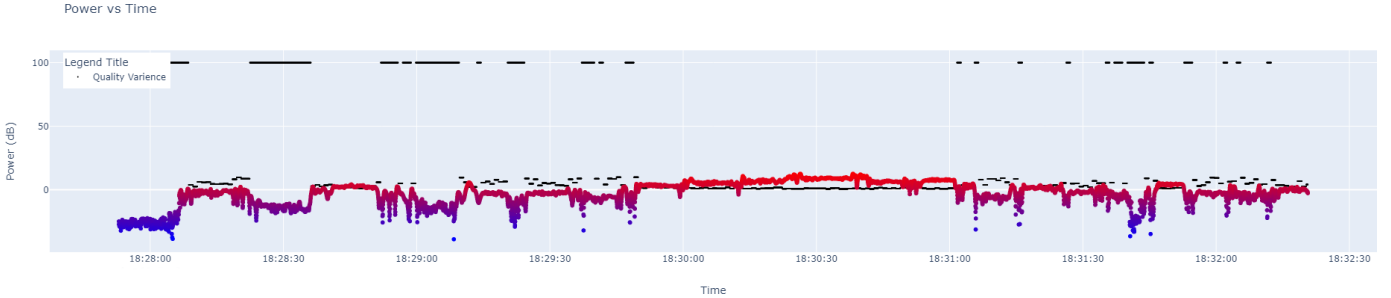


Fig. 3: This figure shows the output of the quality-variance filter along with the signal intensity given from the AERPAW narrowband channel sounder script. This data was collected in a lab setting that resembles the AERPAW setup without any RF front end. The receiver was placed on a moving platform, which was moved from 16 ft to 4 ft and then back to 16 ft from the transmitter. This figure is adapted from Fig. 4.2f of [5].

be rejected as invalid samples and excluded from the GP. However, this threshold needed to be determined at flight time due to limited empirical data. Laboratory testing also indicated that receiver movement influenced the signal's tendency to encounter noise. The binning of the quality metric in a lab setup where the receiver periodically moves towards and away from the transmitter is shown in Figure 3.

A final AERPAW deployment was then created to perform emulation testing and for the final deployment on AERPAW. Two grids are created using the latitude and longitude for both the flying boundary and the rover location boundary. The flying boundary grid is then used for all navigational inputs, and the rover's final estimates are given from the second rover grid. Both grids are sampled from the same GP. The drone then takes off to 40 m for the entire trial. Once at the correct altitude, the drone attempts to take the first radio sample binning data for 6 s while stationary and always facing northwest. If the quality-variance of that sample is higher than the threshold, the sample is retaken with an exponentially higher threshold until this first sample is accepted. The drone then flies to three predefined waypoints shown in figure 1. These waypoint samples give a stable GP and BO for autonomous flight. The drone then flies its mission according to the same AF UCB policy chosen in the simulation. Two possible criteria can trigger an auxiliary routine that creates a circle of waypoints from the drone's current position (observing the boundary limits). The first criterion is that the AF has repeatedly chosen very spatially similar points to investigate. This is similar to the simulation ending routine which indicates that drone has estimated it is within close proximity to the channel gain maximum. The second is if the drone rejects a maximum number of measurements throughout the mission. This is a failsafe that was seen to benefit the mission while testing within the AERPAW emulator. If the drone cannot navigate autonomously to points that provide valid radio samples for the GP, a circular routine of waypoints ensures that the radio will be given a broad spatial set of sample locations, which might recover a gradient towards the transmitter. During the mission, a mission timer tracks the duration and logs the final predicted location from the rover grid space for the three- and

ten-minute estimates.

III. RESULTS AND ANALYSIS

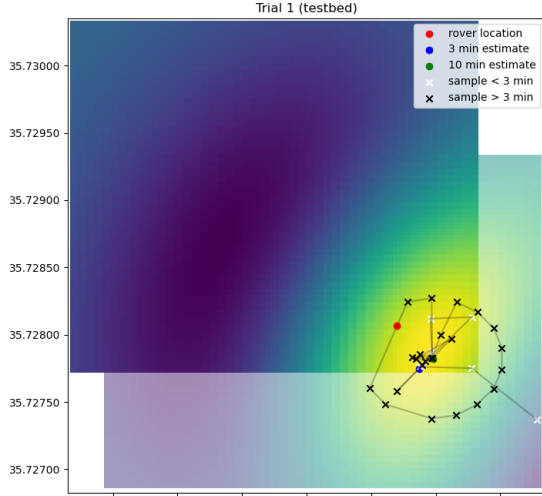
Table I presents the results from the AERPAW emulator and testbed environments. The first mission shows how quickly the GP can fit a transmitter that is relatively close (125 m) from the drone's starting location. However, the drone could not resolve a better 10-minute location estimate due to receiver gain saturation. While a consistently high gain is generally desired for communication, corresponding to an ideal channel, in this case, the signal 'clipping' makes a spatial 'plateau.' This spatial feature makes resolving a transmitter location nearly impossible when within this region. Seeing this within the emulator, the radius for the auxiliary circle was set expecting to encounter this signal behavior; however, in this case, the auxiliary path was not wide enough to provide sufficient localization information. Additionally, critical points were missed on the northwest side of the auxiliary path due to excessive noise, correctly excluded by the quality-variance filter.

The second trial, shown in Figure 4b, gives the team's best 10-minute result of 27.8 m. The 3-minute result did not provide quite enough time for the drone to establish a proper gradient and travel to the transmitter 330 m from takeoff. However, the drone was able to establish a proper optimal trajectory toward the transmitter and perform the auxiliary path maneuver while staying within the boundary conditions. The auxiliary path was wide enough to provide additional localization to the GP, and the quality-variance filter was working appropriately to filter excessive noise. This result shows the ideal behavior of the drone in this situation. To provide a better three-minute GP estimate with this starting routine, a kernel that supplied more information about the signal from this starting distance (as a prior) would need to be considered.

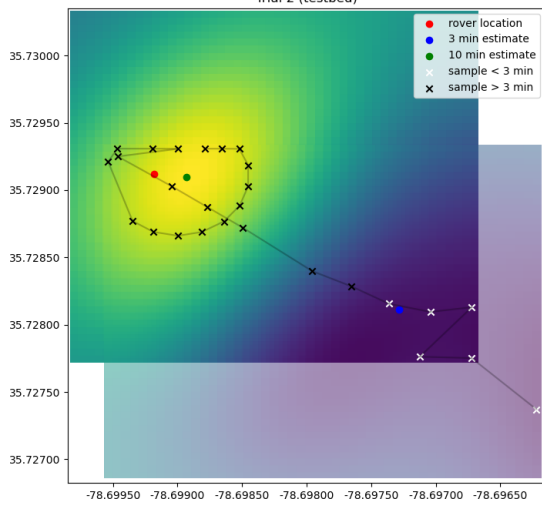
During the third trial, the drone encountered a confluence of issues, which resulted in degraded localization estimation performance. However, the mission was not a failure; the drone was able to produce locations for both timed estimates from a starting distance of 286 m. Log analysis revealed that the quality-variance filter threshold (set with the first sample) was

TABLE I: The three-run simulation and testbed results. The bracketed number indicates the trial number corresponding to the hidden locations given in Figure 1.

3-min (T.1)	3-min (T.2)	3-min (T.3)	3-min Average	10-min (T.1)	10-min (T.2)	10-min (T.3)	10-min Average
Simulation Results							
71.7m	265m	174m	170.23m	52.8m	17m	19m	29.6m
Testbed Results							
40.5m	239.1m	232.4m	170.7m	41.6m	27.8m	130.4m	66.6m



(a)



(b)

Fig. 4: This figure shows a reconstruction of the final Gaussian process estimate for the first and second run, along with the actual rover location shown as a red dot. The green dot shows the final ten-minute estimate, and the blue dot indicates the three-minute estimate. This GP reconstruction uses the final kernel hyperparameters indicated by the vehicle log. Part of this figure is adapted from Fig. 4c of [7].

set to exclude any variance above 35. This was different from the second run, which allowed samples with a less strict value of 67. This disallowed many of the first critical direction-finding waypoints from being included within the GP. The

drone then generated the auxiliary path due to missing too many sample measurements. From this waypoint path two samples were accepted. These samples greatly increased the accuracy of the location estimate. The drone reestablished an optimal path but was unable to collect any more samples due to the time limit.

IV. CONCLUSION

The results of the three trials show significant robustness in the GP and BO architecture for drone-based location finding. The quality-variance filter identified and removed outlier noise values from the narrowband receiver. Unfortunately, the drone was unable to find the correct filter parameter value from the start of the third trial. This alone shows a necessity for improved performance of the AERPAW emulator and a need for radio data collection. If the emulation noise and the testbed had a reliable digital-twin agreement, the filter parameter could be safely studied and set within the emulator similar to the auxiliary path area. This would save mission time and prevent mission hazardous calibrations.

REFERENCES

- [1] D. Romero and S.-J. Kim, “Radio Map Estimation: A data-driven approach to spectrum cartography,” *IEEE Signal Process. Mag.*, vol. 39, no. 6, pp. 53–72, Nov. 2022, doi: 10.1109/SP.2022.3200175.
- [2] R. Shrestha *et al.*, “Radio Map Estimation in the Real-World: Empirical Validation and Analysis,” in *IEEE Conference on Antenna Measurements and Applications*, pp. 169–174, 2023.
- [3] H. Kwon and I. Guvenc, “RF Signal Source Search and Localization Using an Autonomous UAV with Predefined Waypoints,” in *2023 IEEE 97th Vehicular Technology Conference (VTC2023-Spring)*, Jun. 2023, pp. 1–6. doi: 10.1109/VTC2023-Spring57618.2023.10200783.
- [4] G. Matz and F. Hlawatsch, “Fundamentals of Time-Varying Communication Channels,” in *Wireless Communications Over Rapidly Time-Varying Channels*. Elsevier, pp. 1–63, 2021.
- [5] P. Kudyba, “Rapid Autonomous Narrow-band Wireless Localization via Gaussian Process and Bayesian Optimization”, M.S. thesis, Sch. of Electr. and Comput. Eng., University of Georgia, Athens, GA, June 2024.
- [6] V. Marojevic *et al.*, “Advanced wireless for unmanned aerial systems: 5g standardization, research challenges, and aerpaw architecture,” *IEEE Vehicular Technology Magazine*, vol. 15, no. 2, pp. 22–30, 2020.
- [7] P. Kudyba *et al.*, “A UAV-assisted wireless localization challenge on AERPAW” submitted for publication in *IEEE Communications Magazine*, Special Call on Experimentation in Large-Scale Wireless Community Testbeds, May, 2024.
- [8] C. E. Rasmussen and C. K. I. Williams, Gaussian processes for machine learning, in *Adaptive computation and machine learning*. Cambridge, Mass: MIT Press, 2006.
- [9] M. Santos *et al.*, “Multi-robot Learning and Coverage of Unknown Spatial Fields,” in *International Symposium on Multi-Robot and Multi-Agent Systems*, pp. 137–145, 2021.
- [10] D. Pickem *et al.*, “The Robotarium: A remotely accessible swarm robotics research testbed,” in *IEEE International Conference on Robotics and Automation*. IEEE, pp. 1699–1706, 2017.